N-body interactions between trapped ion qubits via spin-dependent squeezing

Or Katz, ^{1, 2, 3, *} Marko Cetina, ^{1, 3} and Christopher Monroe^{1, 2, 3, 4}

¹Duke Quantum Center, Duke University, Durham, NC 27701

²Department of Electrical and Computer Engineering, Duke University, Durham, NC 27708

³Department of Physics, Duke University, Durham, NC 27708

⁴IonQ, Inc., College Park, MD 20740

(Dated: February 10, 2022)

We describe a simple protocol for the single-step generation of N-body entangling interactions between trapped atomic ion qubits. We show that qubit state-dependent squeezing operations and displacement forces on the collective atomic motion can generate full N-body interactions. Similar to the Mølmer-Sørensen two-body Ising interaction at the core of most trapped ion quantum computers and simulators, the proposed operation is relatively insensitive to the state of motion. We show how this N-body gate operation allows the single-step implementation of a family of N-bit gate operations such as the powerful N-Toffoli gate, which flips a single qubit if and only if all other N-1 qubits are in a particular state.

The central ingredient in a quantum computer is the controllable quantum entanglement of its degrees of freedom, allowing the system to evolve over an exponentially large state space that can encode certain problems that are otherwise intractable. The qubit and gate model of a quantum computer employs a universal set of operations, such as single-qubit rotations and two-qubit controlled-NOT gates [1]. While such few-qubit interactions are sufficient for general computation, and can be used to construct many-body entangled states [2– 6, many-gubit interactions can dramatically simplify quantum circuit structures, speed up their execution, and extend the power of quantum computer systems facing decoherence. For example, direct N-qubit operations such as the N-qubit Toffoli gate [7] are expected to find native use in quantum adders and multipliers [8], Grover searches [9–11], error-correction encoding [12– 14, variational quantum algorithms for calculating electronic properties of molecules and materials [15–17], and simulations of nuclear structure and lattice gauge theories [18, 19].

Quantum gates based on many-body interactions have been proposed in several leading physical quantum platforms, from trapped ions [10, 20–22] and neutral atoms [23–27] to superconducting systems [26, 28]. Here we concentrate on trapped ion qubits, which feature a high degree of control, very long qubit coherence times, high quantum gate fidelities and dense qubit connectivity [29–31]. There have been proposals to realize N-body interactions between trapped ions using photons controlled by external optical cavities [21] or phonons underlying the Coulomb-coupled motion of the ions [10, 20, 22]. All of the above proposals rely on either having N or more steps, special auxiliary qubit level structures, or exquisite control or pure-state preparation of the mediating phonons/photons.

Here we discover a simple single-step protocol for N-body entangling interactions between trapped ion qubits or effective spins. The operation is similar to the workhorse Mølmer-Sørensen (MS) two-body interaction [32–35], which relies upon gubit state-dependent displacement forces. We show instead, that statedependent squeezing forces can generate tunable Nbody interactions between the qubits. We further demonstrate construction of the N-Toffoli gate in a single step, and discuss other classes of N-body spin Hamiltonians that can be similarly generated. As in the standard two-qubit MS protocol [10, 32–35], this scheme does not rely on a pure initial phonon state and can be relatively insensitive to thermal motion. (We note that spin-independent motional squeezing has recently been used to enhance MS gate performance, but without changing the form of the underlying two-body interaction [36–38].)

The central idea behind trapped ion quantum gates is the coupling between spins and motion (phonons) through spin-dependent forces [20, 32–35], as illustrated in Fig. 1. Owing to the Coulomb interaction between the trapped ions, their motion around equilibrium can be expressed by collective normal modes of harmonic oscillation. We focus on the coupling through a single phonon mode through a near-resonance driving force, although generalization to multiple modes is straightforward [41, 42]. We represent the phonon state of mode min a frame that rotates at the mode oscillation frequency ω_m using the phase space position and momentum operators $\hat{x}_m = x_m^0(\hat{a}_m^{\dagger} + \hat{a}_m)$ and $\hat{p}_m = ip_m^0(\hat{a}_m^{\dagger} - \hat{a}_m)$. Here, $\hat{a}_m^{\dagger}(\hat{a}_m)$ are the bosonic creation (annihilation) operators and $x_m^0 = \sqrt{\hbar/2M\omega_m}$ $(p_m^0 = \sqrt{\hbar M\omega_m/2})$ are the zero-point spread in position (momentum) associated with mode m, where M is the mass of a single ion. The spin-motion coupling is parametrized by the Lamb-Dicke parameter $\eta_{im} = b_{im}\eta_m$, where $\eta_m = kx_m^0$, k is the effective wavenumber of the radiation field driving the motion [39] and b_{im} is the mode participation ma-

 $^{^{*}}$ Corresponding author: or.katz@duke.edu

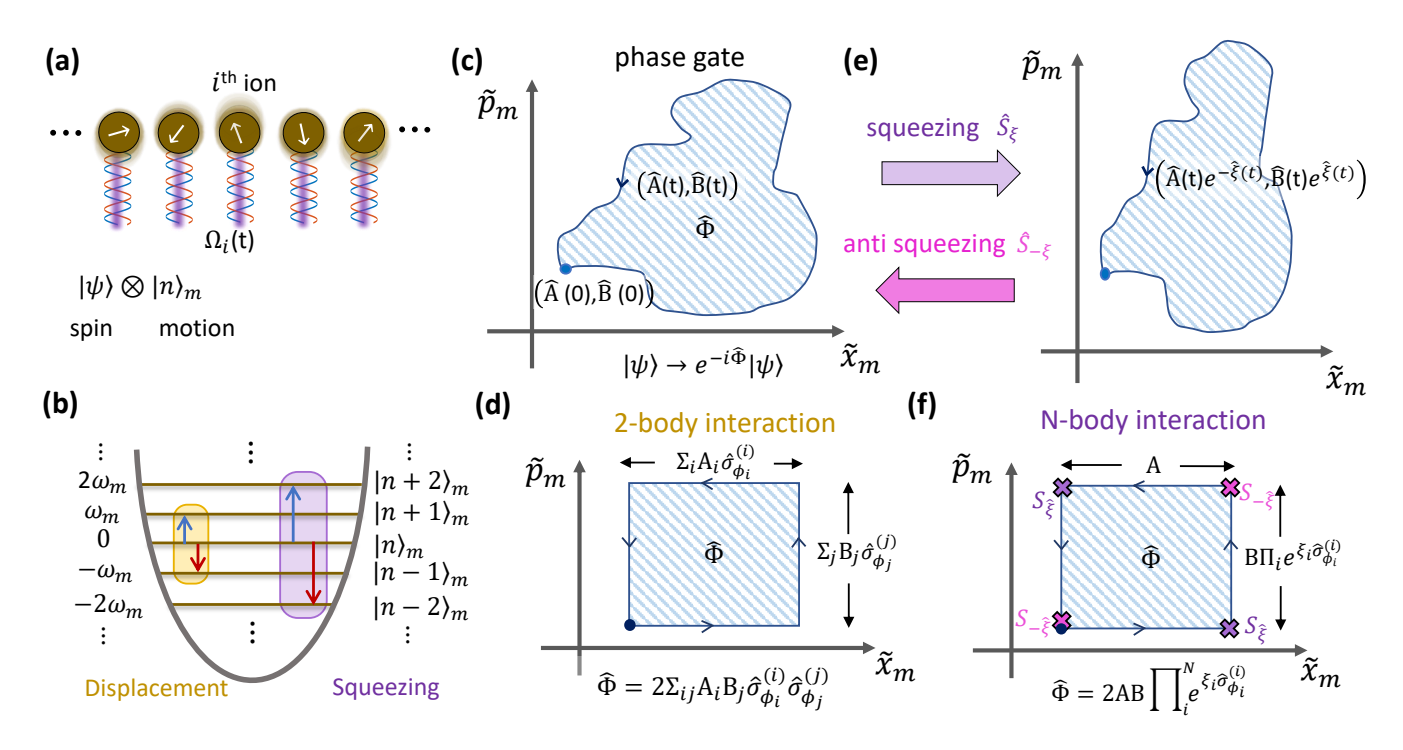


Figure 1. Quantum Phase Gates with trapped ions. (a) A chain of trapped ions whose many-body spin state $|\psi\rangle$ is decoupled from the motional state $|n\rangle_m$ of a single harmonic phonon mode m represented by vibrational integer index $n \geq 0$. Ions are addressed with bi-chromatic Laser fields with carrier spin-flip Rabi rates Ω_i . (b) Motional sideband transitions driven by the laser field. Tuning the laser field on resonance with the first red and blue sideband transitions at frequency $\pm \omega_m$ from the carrier [39] generates a spin-dependent force through the absorption and emission phonons. Tuning the tones at the second red and blue sidebands at $\pm 2\omega_m$ from the carrier generates spin-dependent squeezing by absorption and emission of pairs of phonons. (c) Displacing the motion of mode m in a closed loop of phase space adds a phase $\hat{\Phi}$ to the quantum state that is given by the area of the enclosed contour. (d) The MS gate using spin-dependent displacements result in a spin-dependent phase linear in the spin operators. When applied to multiple ions, the resulting phase $\hat{\Phi}$ is thus quadratic in the spin operators, corresponding to 2-body MS interaction [35, 40]. (e) Motional-squeezing shrinks one direction in phase space but expands the other to conserve the phase space element area. (f) N-body entangling gate. Synchronized spin-dependent squeezing (cross symbols) applied in between displacements produces squeezing of the motion along momentum axis. The phase $\hat{\Phi}$ now depends exponentially on the spins, and therefore contains products of N spin operators. The phase space axes are displayed with dimensionless units $\tilde{x}_m = \hat{x}_m/(2x_m^0)$ and $\tilde{p}_m = \hat{p}_m/(2p_m^0)$, with the convention $[\tilde{x}_m, \tilde{p}_m] = i/2$.

trix between ion i and mode m, with $\sum_i b_{im}b_{in} = \delta_{nm}$ and $\sum_m b_{im}b_{jm} = \delta_{ij}$.

The MS interaction arises by addressing multiple ions on the first red and blue sidebands of mode m from the spin-flip carrier, with relative phase $\delta\phi_i$ and zero-point Rabi rate $\eta_{im}\Omega_i(t)$ for ion i. Here the carrier Rabi frequency $\Omega_i(t)$ is proportional to the drive strength, and we assume the motion is confined within the Lamb-Dicke regime where $\eta_{im}\langle\hat{a}_m^\dagger+\hat{a}_m\rangle\ll 1$ [39]. This spin-dependent force displaces the phonon state in phase space by position $\hat{A}(t)=\sum_i A_i(t)\hat{\sigma}_x^{(i)}$ and momentum $\hat{B}(t)=\sum_i B_i(t)\hat{\sigma}_x^{(i)}$, where $\hat{\sigma}_x^{(i)}$ are the Pauli spin flip operators (chosen uniformly along x for convenience), and the position and momentum displacement amplitudes are $A_i(t)=\frac{1}{2}\eta_{im}\int_0^t dt'\Omega_i\sin\delta\phi_i$ and $B_i(t)=\frac{1}{2}\eta_{im}\int_0^t dt'\Omega_i\cos\delta\phi_i$ [32]. Note we have scaled the position (momentum) variables by $2x_m^0(2p_m^0)$.

Geometric phase gates such as the MS gate displace the ions in closed phase space loops [Fig. 1(c) and (d)]. By the end of the gate at time T, the spin state of the ions is decoupled from the phonons but has evolved according to $U_{\rm MS}(T) = e^{-i\hat{\Phi}}$, with geometrical phase operator

$$\hat{\Phi} = -2 \int_0^T \hat{\mathbf{B}}(t) \frac{d\hat{\mathbf{A}}(t)}{dt} dt. \tag{1}$$

Because $\hat{A}(t)$ and $\hat{B}(t)$ are linear in the spin operators, the gate phase operator $\hat{\Phi}$ is quadratic in the spin operators [43, 44], limiting the standard MS gate to just two-body (Ising) interactions.

To generate an N-body spin interaction, we now consider the effect of spin-dependent motional squeezing on a phase gate operation. Spin-dependent squeezing can be generated by driving the second red and blue sidebands of a single phonon mode m, as shown in Fig. 1(b)

[39]. Setting the zero-point $2^{\rm nd}$ sideband Rabi rates equal to $\eta_{im}^2\Omega_i/2$ and the relative phase between the drives constant across the chain $(\delta\phi_i = \delta\phi)$, the spin-motion interaction becomes (in the Lamb-Dicke regime),

$$H_S = \frac{i\hbar}{4} \left(e^{i\delta\phi} \hat{a}_m^2 - e^{-i\delta\phi} \hat{a}_m^{\dagger 2} \right) \sum_{i=1}^N \eta_{im}^2 \Omega_i \hat{\sigma}_{\phi_i}^{(i)}. \tag{2}$$

Here $\hat{\sigma}_{\phi_i}^{(i)} \equiv \hat{\sigma}_x^{(i)} \cos \phi_i + \hat{\sigma}_y^{(i)} \sin \phi_i$ is the Pauli spin-flip operator of spin i set by the average phase ϕ_i of the i^{th} pair of drives. The phonon operator in Eq. (2) is the generator of quadrature squeezing along the axis rotated by $\delta\phi/2$ and anti-squeezing along $(\pi + \delta\phi)/2$. Setting $\delta\phi = 0$ squeezes phase-space in position and anti-squeezes in momentum whereas $\delta\phi = \pi$ does the opposite. For simplicity, we fix $\delta\phi = 0$ throughout the paper. Under the time-dependent Hamiltonian H_S of Eq. (2), the quantum state evolves by the spin-dependent squeezing operator

$$S_{\hat{\xi}}(t) = e^{\frac{1}{2}\hat{\xi}(t)(\hat{a}_m^2 - \hat{a}_m^{\dagger 2})},\tag{3}$$

where the spin-dependent squeezing amplitude is

$$\hat{\xi}(t) = \sum_{i} \xi_{i}(t)\hat{\sigma}_{\phi_{i}}^{(i)} = \frac{1}{2} \sum_{i} \hat{\sigma}_{\phi_{i}}^{(i)} \eta_{im}^{2} \int_{0}^{t} \Omega_{i}(\tau) d\tau.$$
 (4)

To illustrate the effect of squeezing on a phase gate operation, we first consider an alternating sequence of spin-dependent squeezing operations and displacement forces, here assumed to be spin-independent. Specifically, we apply four discrete displacements along a rectangular-shaped closed-loop in phase space [35] interspersed with four alternating squeezing operators applied at the corners of the rectangle that ultimately decouple the motion, as depicted in Fig. 1(f). The displacements in position $\hat{\mathbf{A}}(t_x) = \mathbf{A}\mathbb{1}$ and momentum $\hat{\mathbf{B}}(t_p) = \mathbf{B}\mathbb{1}$ are applied for times t_x and t_p , respectively, where $\mathbf{A} = \sum_i A_i(t), \mathbf{B} = \sum_i B_i(t)$ and $\mathbb{1}$ is the identity spin operator. The squeezing operators are interspersed with spin-dependent squeezing amplitude $\hat{\xi}(t_S)$ for time t_S , for a total gate time of $T = 4t_S + 2t_x + 2t_p \approx 4t_S$. The evolution operator of this sequence is written

$$U_{\text{seq}}(T) = S_{\hat{\xi}}^{\dagger} D(-iB) S_{\hat{\xi}} D(-A) S_{\hat{\xi}}^{\dagger} D(iB) S_{\hat{\xi}} D(A)$$
(5)
$$= D(-iBe^{\hat{\xi}}) D(-A) D(iBe^{\hat{\xi}}) D(A)$$
(6)
$$= e^{-i\hat{\Phi}_{\text{seq}}},$$
(7)

where $D(\alpha) = e^{\alpha \hat{a}_m^{\dagger} - \alpha^* \hat{a}_m}$ is the displacement operator, which moves the phonon state in phase space by $2x_m^0 \operatorname{Re}(\alpha)$ along the \hat{x}_m coordinate and by $2p_m^0 \operatorname{Im}(\alpha)$ along \hat{p}_m . The squeezing operations produce a net displacement whose magnitude is dilated or contracted depending on the spin, since $S_{\hat{\xi}}^{\dagger} D(i\operatorname{B}) S_{\hat{\xi}} \equiv D(i\operatorname{Be}^{\hat{\xi}})$. Because $\hat{\xi}$ is linear in the spin operators from Eq. (4), the

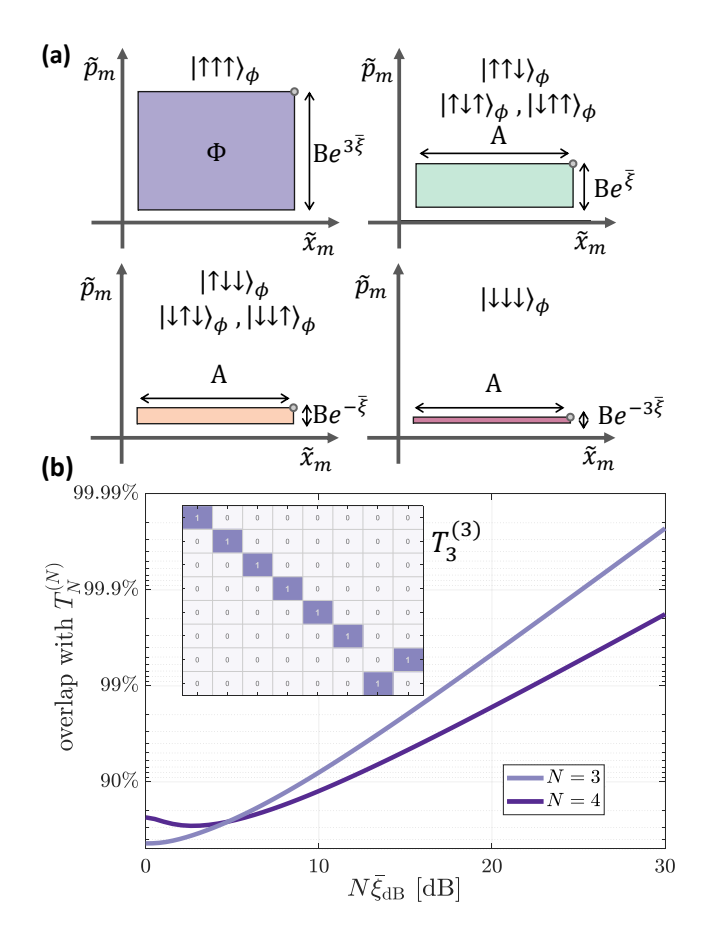


Figure 2. 3-body entangling gates. (a) Phase space evolution for three spins, following the sequence of alternating spin-independent displacements and spin-dependent squeezing operations [c.f. Fig. 1(f) and Eq. (5)]. Each ion squeezes (anti-squeezes) the momentum quadrature of the mth motional mode by a factor $e^{-\bar{\xi}}$ ($e^{\bar{\xi}}$) if its spin points downwards (upwards). The state-dependent phase-space area $\hat{\Phi}_{\rm seq}$ accumulated in the evolution generates the gate $U_{\rm seq} = e^{-i\hat{\Phi}_{\rm seq}}$ with a maximal squeezing of the oscillator mode by a factor $e^{N\bar{\xi}}$ when all spins are aligned. (b) Overlap between the proposed many-body gate in Eq. (8) (accompanied by single-qubit rotations on the third qubit as described in the main text) and the N-Toffoli gate $T_N^{(N)}$ depending on the maximal squeezing of phase-space area in dB ($\bar{\xi}_{dB} = 10\bar{\xi} \log_{10} e$) for N=3,4. Inset: ideal $T_3^{(3)}$ operator in the computational basis.

gate phase operator is *exponential* in the spin operators:

$$\hat{\Phi}_{\text{seq}} = 2ABe^{\hat{\xi}} = 2AB \prod_{i=1}^{N} \left(\mathbb{1} \cosh \xi_i + \hat{\sigma}_{\phi_i}^{(i)} \sinh \xi_i \right),$$
(8)

corresponding to an effective N-body Hamiltonian $H_{\rm eff} = \hbar \hat{\Phi}_{\rm seq}/T$. This remarkable construction features many-body in interaction terms, where the relative contribution of the N-body term scales as $\prod_i \tanh \xi_i$, which is sizeable for $\xi_i \gtrsim 1$.

In the limit $\xi_i \gg 1$, the gate phase operator becomes

$$\hat{\Phi}_{\text{seq}} \to 2ABe^{N\bar{\xi}} \prod_{i=1}^{N} \frac{1}{2} \left(\mathbb{1} + \hat{\sigma}_{\phi_i}^{(i)} \right), \tag{9}$$

where $\bar{\xi} = \sum_i \xi_i/N$ is the mean squeezing amplitude of the spins. Eq. (9) is proportional to the projection operator on the state $|\uparrow_{\phi} \cdots \uparrow_{\phi}\rangle$, in which each spin points upward along an eigenstate of $\hat{\sigma}_{\phi_i}^{(i)}$. This renders $U_{\rm seq}$ into the N-qubit controlled-phase gate, which appends the phase factor $\exp(-2i{\rm AB}e^{N\bar{\xi}})$ to the state $|\uparrow_{\phi} \cdots \uparrow_{\phi}\rangle$. From here, it is easy to construct the N-bit Toffoli gate $T_N^{(n)}$, which flips qubit n if and only if all other N-1 qubits point up along $\hat{\sigma}_{\phi_i}^{(i)}$ [7, 20]. By setting $2{\rm AB}e^{N\bar{\xi}}=\pi$ and surrounding this operation by single-qubit $\pi/2$ rotations on qubit n, we find $T_N^{(n)}=R_z^{(n)}(\pi/2)U_{\rm seq}R_z^{(n)}(-\pi/2)$. We illustrate the phase space trajectories of the many-

We illustrate the phase space trajectories of the many-body quantum gate for N=3 qubits in Fig. 2a for $\xi_i=\bar{\xi}$. The phase accumulated by the quantum state depends exponentially on the number of spins that are in the state $|\uparrow_{\phi}\rangle$. In Fig. 2(b) (inset) we exemplify the operation of the 3-Toffoli gate $(T_3^{(3)})$ on three qubits in the computational basis. We find that the overlap [45] of the proposed gate \tilde{U}_{seq} with the ideal Toffoli gate increases as the maximal degree of squeezing of the oscillator mode is increased and plot the overlap for N=3,4.

We next generalize this result and show that various N-body Hamiltonians can be generated by simultaneous application of displacements and spin-dependent squeezing. Displacements are generated in the interaction picture by the Hamiltonian

$$H_D = 2x_m^0 \hat{\alpha}(t)\hat{p}_m - 2p_m^0 \hat{\beta}(t)\hat{x}_m.$$
 (10)

where the forces $\hat{\alpha}, \hat{\beta}$ are Hermitian, and their spindependence is determined by the underlying mechanism from which they are produced. For example, fields produced by the trap's electrodes couple to the ions' charge and can generate state-independent displacements [29], whereas optical dipole forces [46–48] or near-field microwave fields [49, 50] can generate displacements linear in the spin operators.

The total Hamiltonian of the system is then given by $H(t) = H_S(t) + H_D(t)$, and the total evolution operator can be represented in time-ordered form [51]

$$U(t) = S_{\hat{\xi}}(t)U_D(t). \tag{11}$$

The operator U_D describes the contribution of phasespace displacements to the evolution and is generated by the Hamiltonian

$$H'_{D} = S_{\hat{\xi}}^{\dagger} H_{D} S_{\hat{\xi}} = 2x_{m}^{0} \hat{\alpha}(t) e^{\hat{\xi}(t)} \hat{p}_{m} - 2p_{m}^{0} \hat{\beta}(t) e^{-\hat{\xi}(t)} \hat{x}_{m},$$
(12)

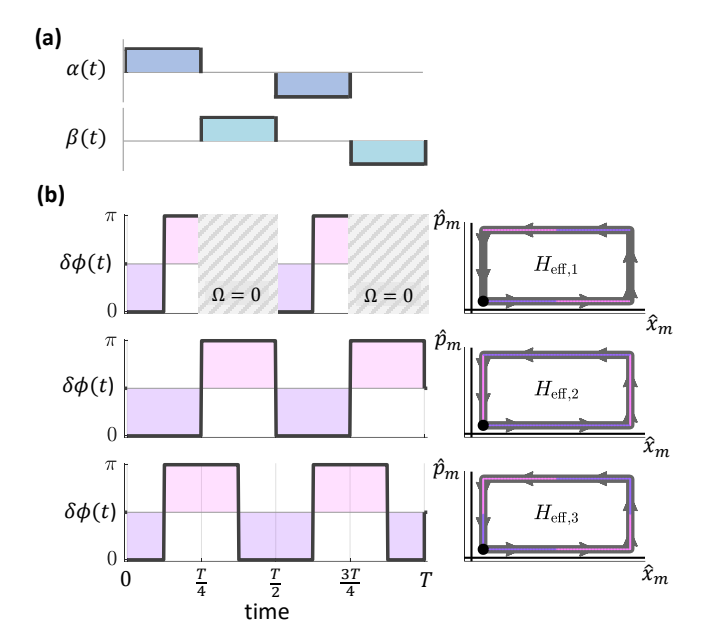


Figure 3. Sample sequences of simultaneous displacement and squeezing to generate N-body spin Hamiltonians. (a) Spin-independent forces $\alpha(t)$ and $\beta(t)$ displace the motion of a single mode along the position and momentum quadratures, respectively. (b) Sequences of discrete modulation of $\delta\phi$, the relative phase of the red and blue tones, alternate between squeezing (anti-squeezing) of the \hat{x}_m quadrature for $\delta\phi=0$ ($\delta\phi=\pi$). At the end of each sequence, any correlations developed between motion and spins during the evolution are erased, manifesting the evolution by an effective spin Hamiltonian $H_{\rm eff,1},\,H_{\rm eff,2}$ or $H_{\rm eff,3}$ described in the main text. Grey shaded area indicate regions in which the beam is turned off $\Omega(t)=0$.

provided that $\hat{\alpha}, \hat{\beta}$ and $\hat{\xi}$ commute at all times during the gate. Spin-dependent squeezing thus renders the standard forces $\hat{\alpha}, \hat{\beta}$ as nonlinear in the spin operators, via the exponential terms $e^{\pm \hat{\xi}(t)}$ in Eq. (12). Yet, the evolution of U_D is identical to that of the MS gate under the simple transformation $\hat{\alpha} \to \hat{\alpha} e^{\hat{\xi}}, \hat{\beta} \to \hat{\beta} e^{-\hat{\xi}}$ and is therefore described by [40]

$$U_D(t) = e^{-i\hat{\Phi}} D(i\hat{B}) D(\hat{A}). \tag{13}$$

The phase operator $\hat{\Phi}(T)$ is given by Eq. (1) and the Hermitian phase-space displacements are

$$\hat{\mathbf{A}}(t) = \int_0^t e^{\hat{\xi}(t')} \hat{\alpha}(t') dt',$$

$$\hat{\mathbf{B}}(t) = \int_0^t e^{-\hat{\xi}(t')} \hat{\beta}(t') dt'.$$
(14)

Similar to the MS gate, the operator U in Eq. (11) entangles the internal spin state with the motional state during the gate operation. To realize a gate that is

independent of motion for all input states, we require that at t = T,

$$\hat{A}(T) = \hat{B}(T) = \hat{\xi}(T) = 0.$$
 (15)

This decouples the motion (both in displacement and squeezing) so that the net evolution operator contains only spin operators, yielding $U(T) = e^{-i\hat{\Phi}}$.

We now present sample sequences of simultaneous squeezing and spin-independent displacements that produce various N-body spin Hamiltonians. The sequences we consider follow a rectangular-shaped trajectory in phase space given by

$$\hat{\alpha}(t) = \mathbb{1}\alpha(t) = \frac{4}{T} \left[w(t, 0, \frac{T}{4}) - w(t, \frac{T}{2}, \frac{3T}{4}) \right] \quad (16)$$

$$\hat{\beta}(t) = \mathbb{1}\beta(t) = \frac{4}{T} \left[w(t, \frac{T}{4}, \frac{T}{2}) - w(t, \frac{3T}{4}, T) \right]$$
 (17)

where $w(t,t_0,t_1)$ is the rectangular window function returning 1 if $t_0 \leq t < t_1$ and zero otherwise. For the squeezing operation, we assume constant Rabi frequencies Ω_i but alternate $\delta\phi(t)$ between the two binary values 0 and π , yielding $\xi_i(t) = \frac{1}{2}\eta_{im}^2\Omega_i\int_0^t e^{i\delta\phi(t')}dt'$. In Fig. 3(b), we display three different sequences

In Fig. 3(b), we display three different sequences that satisfy the spin/motion disentanglement conditions of Eqs. (15) and generate three effective spin-Hamiltonians. The first sequence (Fig. 3(b) top) squeezes only during displacements along \hat{x}_m (the squeezing beam is turned off in the grey shaded area), yielding

$$H_{\text{eff},1} = 2\sum_{k=0}^{\infty} \frac{\hat{J}_{\phi}^{k}}{(k+1)!} \simeq 2\hat{J}_{\phi}^{-1} \left(e^{\hat{J}_{\phi}} - \mathbb{1}\right),$$
 (18)

where the collective spin operator is

$$\hat{J}_{\phi} = \frac{T}{16} \sum_{i} \eta_{im}^2 \Omega_i \hat{\sigma}_{\phi_i}^{(i)}. \tag{19}$$

The Hamiltonian is composed of an infinite series of powers of \hat{J}_{ϕ} . The approximate form in Eq. (18) is an equivalent convergent representation of the sum for invertible \hat{J}_{ϕ} . The second sequence (Fig. 3(b) middle) generates the spin Hamiltonian

$$H_{\text{eff},2} = \sum_{k=0}^{\infty} \frac{\hat{J}_{\phi}^{2k}}{(2k+21)!} \simeq 2\hat{J}_{\phi}^{-2} \sinh^{2}(\hat{J}_{\phi}), \qquad (20)$$

which contains only even powers of \hat{J}_{ϕ} , and the third sequence (Fig. 3(b) bottom) generates $H_{\rm eff,3} = \left(H_{\rm eff,1}\right)^2/2$.

We now consider the speed of the N-body gate, especially given that it relies on $2^{\rm nd}$ order motional sidebands, which in the Lamb-Dicke limit are considerably weaker than the $1^{\rm st}$ order sidebands in the conventional MS gate. For two-body MS gates through single mode m [40], the gate time can be as short as

 $T_{MS} \approx \pi \sqrt{N}/(\eta_m \Omega)$, where the Rabi frequency Ω is taken to be uniform over the involved ions. The N-body gate presented here based on resonant spin-dependent squeezing gives a gate time of $T \approx 8N\bar{\xi}/(\Omega\eta_m^2)$. Here we have assumed that the mode participation scales as $b_{im} \sim 1/\sqrt{N}$, although if modes are more localized, the gates can be tailored to be faster for certain subsets of ions

Our analysis focuses on the interactions generated via resonant coupling with a single phonon mode. However, spin-dependent squeezing through 2nd sidebands can also drive off-resonant sidebands on pairs of modes μ, ν detuned by $\Delta_{\mu\nu} = 2\omega_m - \omega_\mu - \omega_\nu$. This results in multi-mode squeezing in a potentially dense sideband spectrum, with the possibility of neardegeneracies. These off-resonant couplings can be suppressed by judiciously shaping the axial ion trap potential and choosing the target mode so that the unwanted sidebands are sufficiently far from the desired squeezing sideband. For example, the lowest frequency (zig-zag) radial normal mode is relatively isolated, and the resulting off-resonant coupling with the nearest 2nd sideband detuned $\Delta_{\mu m}$ from the drive scales with rate $\frac{1}{4}\sum_{i}\eta_{i\mu}^{2}\eta_{im}^{2}\Omega_{i}^{2}/\Delta_{\mu m}$, while the desired squeezing interaction rate scales as $\eta_m^2 \Omega/(2N)$. Thus the gate error probability is expected to be $\epsilon = \eta_m^2 \Omega/(2N\Delta_{\mu m})$ and can be made small by ensuring $\eta_m^2 \Omega/N \ll \Delta_{\mu m}$. By shaping the mode spectrum such that $\Delta_{\mu m} \sim \mathcal{B}/N$ for instance, where \mathcal{B} is the bandwidth of modes, we find that for fixed Ω , the error from off-resonant excitations does not grow with N. We finally note that it is possible to apply pulse-shaping techniques to control all multimode squeezing operations for the N-body gate operation while decoupling all motional modes, exactly has been demonstrated for multimode MS gates [41, 42].

We finally note that the emergence of N-body interactions discovered here can be seen from the expanded Lie algebra generated by the combined squeezing and displacement Hamiltonians. This is evident from the Magnus expansion representation of the evolution operator [52], a sequence of nested commutators of the Hamiltonian with itself. For the MS interaction, the series terminates after the second term because $[\hat{x}_m, \hat{p}_m] = i\hbar$. Here instead, the series does not terminate because for instance $[(\hat{a}_m^2 - \hat{a}_m^{\dagger 2})\hat{\sigma}_x^{(i)}, \hat{x}_m] = 2\hat{x}_m\hat{\sigma}_x^{(i)}$, thus carrying products of further spin operators along in the expansion. This interaction thus represents a new degree of freedom in controlling trapped ion quantum states, and may significantly expand the expression of trapped ion quantum logic operations.

ACKNOWLEDGMENTS

This work is supported by the ARO through the IARPA LogiQ program; the NSF STAQ program; the

DOE QSA program; the AFOSR MURIs on Dissipation Engineering in Open Quantum Systems, Quantum Measurement/Verification, and Quantum Interactive Protocols; and the ARO MURI on Modular Quantum Circuits.

- [1] M. A. Nielsen and I. L. Chuang, *Quantum Computation and Quantum Information* (Cambridge University Press, Cambridge, UK, 2000).
- [2] C. A. Sackett, D. Kielpinski, B. E. King, C. Langer, V. Meyer, C. J. Myatt, M. Rowe, Q. A. Turchette, W. M. Itano, D. J. Wineland, and C. Monroe, Nature 404, 256 (2000).
- [3] T. Monz, K. Kim, W. Hänsel, M. Riebe, A. Villar, P. Schindler, M. Chwalla, M. Hennrich, and R. Blatt, Phys. Rev. Lett. 102, 040501 (2009).
- [4] T. Monz, P. Schindler, J. T. Barreiro, M. Chwalla, D. Nigg, W. A. Coish, M. Harlander, W. Hänsel, M. Hennrich, and R. Blatt, Phys. Rev. Lett. 106, 130506 (2011).
- [5] A. Omran, H. Levine, A. Keesling, G. Semeghini, T. T. Wang, S. Ebadi, H. Bernien, A. S. Zibrov, H. Pichler, S. Choi, et al., Science 365, 570 (2019).
- [6] C. Song, K. Xu, H. Li, Y.-R. Zhang, X. Zhang, W. Liu, Q. Guo, Z. Wang, W. Ren, J. Hao, H. Feng, H. Fan, D. Zheng, D.-W. Wang, H. Wang, and S.-Y. Zhu, Science 365, 574 (2019).
- [7] T. Toffoli, in Automata, Languages and Programming, edited by J. de Bakker and J. van Leeuwe (Springer, Berlin, Heidelberg, 1980) pp. 632–644.
- [8] V. Vedral, A. Barenco, and A. Ekert, Phys. Rev. A 54, 147 (1996).
- [9] L. K. Grover, in *Proceedings of the twenty-eighth annual* ACM symposium on Theory of computing (1996) pp. 212–219.
- [10] X. Wang, A. Sørensen, and K. Mølmer, Phys. Rev. Lett. 86, 3907 (2001).
- [11] C. Figgatt, D. Maslov, K. A. Landsman, N. M. Linke, S. Debnath, and C. Monroe, Nat. Commun. 8, 1 (2017).
- [12] A. Paetznick and B. W. Reichardt, Phys. Rev. Lett. 111, 090505 (2013).
- [13] A. Y. Kitaev, Annals of Physics 303, 2 (2003).
- [14] M. Müller, K. Hammerer, Y. Zhou, C. F. Roos, and P. Zoller, New J. Phys. 13, 085007 (2011).
- [15] P. J. J. O'Malley et al., Phys. Rev. X 6, 031007 (2016).
- [16] Y. Nam, J.-S. Chen, N. C. Pisenti, K. Wright, C. Delaney, D. Maslov, K. R. Brown, S. Allen, J. M. Amini, J. Apisdorf, et al., npj Quantum Information 6, 1 (2020).
- [17] J. T. Seeley, M. J. Richard, and P. J. Love, J. Chem. Phys. 137, 224109 (2012).
- [18] M. C. Banuls, R. Blatt, J. Catani, A. Celi, J. I. Cirac, M. Dalmonte, L. Fallani, K. Jansen, M. Lewenstein, S. Montangero, et al., Eur. Phys. J. D 74, 1 (2020).
- [19] A. Ciavarella, N. Klco, and M. J. Savage, Phys. Rev. D 103, 094501 (2021).
- [20] J. I. Cirac and P. Zoller, Phys. Rev. Lett. 74, 4091 (1995).
- [21] H. Goto and K. Ichimura, Phys. Rev. A 70, 012305 (2004).

- [22] J. D. Arias Espinoza, K. Groenland, M. Mazzanti, K. Schoutens, and R. Gerritsma, Phys. Rev. A 103, 052437 (2021).
- [23] H. Weimer, M. Müller, I. Lesanovsky, P. Zoller, and H. P. Büchler, Nature Physics 6, 382 (2010).
- [24] L. Isenhower, M. Saffman, and K. Mølmer, Quantum Inf. Process. 10, 755 (2011).
- [25] H. Levine, A. Keesling, G. Semeghini, A. Omran, T. T. Wang, S. Ebadi, H. Bernien, M. Greiner, V. Vuletić, H. Pichler, and M. D. Lukin, Phys. Rev. Lett. 123, 170503 (2019).
- [26] M. Khazali and K. Mølmer, Phys. Rev. X 10, 021054 (2020).
- [27] T. H. Xing, P. Z. Zhao, and D. M. Tong, Phys. Rev. A 104, 012618 (2021).
- [28] E. Zahedinejad, J. Ghosh, and B. C. Sanders, Phys. Rev. Lett. 114, 200502 (2015).
- [29] D. J. Wineland, C. Monroe, W. M. Itano, D. Leibfried, B. E. King, and D. M. Meekhof, J. Res. Nat. Inst. Stand. Technol. 103, 259 (1998).
- [30] K. R. Brown, J. Kim, and C. Monroe, npj Quantum Inf. 2, 16034 (2016).
- [31] T. Lubinski, S. Johri, P. Varosy, J. Coleman, L. Zhao, J. Necaise, C. H. Baldwin, K. Mayer, and T. Proctor, arXiv:2110.03137 (2021).
- [32] K. Mølmer and A. Sørensen, Phys. Rev. Lett. 82, 1835 (1999).
- [33] A. Sørensen and K. Mølmer, Phys. Rev. Lett. 82, 1971 (1999).
- [34] E. Solano, R. L. de Matos Filho, and N. Zagury, Phys. Rev. A 59, R2539 (1999).
- [35] G. Milburn, S. Schneider, and D. James, Fortschritte der Phys. 48, 801 (2000).
- [36] W. Ge, B. C. Sawyer, J. W. Britton, K. Jacobs, J. J. Bollinger, and M. Foss-Feig, Phys. Rev. Lett. 122, 030501 (2019).
- [37] W. Ge, B. C. Sawyer, J. W. Britton, K. Jacobs, M. Foss-Feig, and J. J. Bollinger, Phys. Rev. A 100, 043417 (2019).
- [38] S. Burd, R. Srinivas, H. Knaack, W. Ge, A. Wilson, D. Wineland, D. Leibfried, J. Bollinger, D. Allcock, and D. Slichter, Nature Physics, 1 (2021).
- [39] D. Leibfried, R. Blatt, C. Monroe, and D. Wineland, Rev. Mod. Phys. 75, 281 (2003).
- [40] A. Sørensen and K. Mølmer, Phys. Rev. A 62, 022311 (2000).
- [41] S.-L. Zhu, C. Monroe, and L.-M. Duan, Phys. Rev. Lett. 97, 050505 (2006).
- [42] S. Debnath, N. M. Linke, C. Figgatt, K. A. Landsman, K. Wright, and C. Monroe, Nature 536, 63 (2016).
- [43] Y. Lu, S. Zhang, K. Zhang, W. Chen, Y. Shen, J. Zhang, J.-N. Zhang, and K. Kim, Nature 572, 363 (2019).
- [44] C. Figgatt, A. Ostrander, N. M. Linke, K. A. Landsman, D. Zhu, D. Maslov, and C. Monroe, Nature 572, 368

- (2019).
- [45] We calculate the overlap as the entanglement fidelity of the two Unitary processes. c.f. [53].
- [46] C. Monroe, W. C. Campbell, L.-M. Duan, Z.-X. Gong, A. V. Gorshkov, P. W. Hess, R. Islam, K. Kim, N. M. Linke, G. Pagano, P. Richerme, C. Senko, and N. Y. Yao, Rev. Mod. Phys. 93, 025001 (2021).
- [47] K. A. Gilmore, M. Affolter, R. J. Lewis-Swan, D. Barberena, E. Jordan, A. M. Rey, and J. J. Bollinger, Science 373, 673 (2021).
- [48] P. C. Haljan, K.-A. Brickman, L. Deslauriers, P. J. Lee, and C. Monroe, Phys. Rev. Lett. 94, 153602 (2005).

- [49] T. Harty, M. Sepiol, D. Allcock, C. Ballance, J. Tarlton, and D. Lucas, Phys. Rev. Lett. 117, 140501 (2016).
- [50] R. Srinivas, S. Burd, H. Knaack, R. Sutherland, A. Kwiatkowski, S. Glancy, E. Knill, D. Wineland, D. Leibfried, A. C. Wilson, et al., Nature 597, 209 (2021).
- [51] J. Wei and E. Norman, J. Math. Phys. 4, 575 (1963).
- [52] W. Magnus, Communications on Pure and Applied Mathematics 7, 649 (1954).
- [53] M. Horodecki, P. Horodecki, and R. Horodecki, Phys. Rev. A 60, 1888 (1999).